

## OPTIMAL REGULATORS DESIGN FOR VSC HVDC SYSTEM USING SIMPLEX METHOD

Mazouz Lakhdar<sup>1</sup>, Elbar Mohamed<sup>2</sup>, Boudhief Mohamed<sup>1</sup>,

<sup>1</sup> Renewable Energy Systems Applications Laboratory (LASER), Faculty of Science and Technology, Ziane Achour University, Djelfa 17000, Algeria.

<sup>2</sup> Applied Automation and Industrial Diagnostics Laboratory (LAADI), Faculty of Science and Technology, Ziane Achour University, Djelfa 17000, Algeria.

[l.mazouz@univ-djelfa.dz](mailto:l.mazouz@univ-djelfa.dz) , [m.elbar@univ-djelfa.dz](mailto:m.elbar@univ-djelfa.dz) , [m.boudhief@univ-djelfa.dz](mailto:m.boudhief@univ-djelfa.dz)

**Abstract:** The use of VSC HVDC (voltage source converter for high voltage direct current link) to transmit the power over long distance has lot of technical advantages compared to AC transmission as eradicating of interactions problem that can happen when the AC systems are coupled directly. To achieve wanted objectives from the use of HVDC system, it is necessary to develop the performance of the control system and this passes by selecting good parameters of Proportional – Integral PI regulators used for the control these systems. In this paper simplex optimization method is one of direct methods that can be used for tuning process of the designed PI regulators which consequently ameliorate the control system behavior. The benefit from the use of this method is to get new optimized PI gains with perfect accuracy and in typical speed. PSCAD/ EMTDC simulations are presented to show the performance of the proposed method during response steps and under serious perturbation.

Key words: VSC HVDC; optimization, simplex method, PI regulators

### 1. Introduction

The transport of energy through DC cables can be considered as good way to link between two AC systems and also to transport huge power from remote sources of energy through long distance thanks to their environmental, technological, and financial benefits. Compared to AC transmission and classical HVDC, the new DC systems based on IGBT element offers lot of benefits as the independent control of the active and reactive power in each side thanks to the use of PWM converters and also there is no communication between the two stations. Another advantage is that the VSC converter can create its own voltage without the presence of rotating machines and also it is not necessary to introduce AC filters contrary to conventional HVDC systems. The VSC can be used to remove or inject the reactive power in the connected network and the commutations between valves are instantaneously because of the IGBT element use. Finally VSC HVDC transmission is becoming today as good key to connect the remote offshore wind farms to the land thanks to their technical advantages as the small size of offshore converter station and the absence of filters because of PWM converters use.

For good operating of VSC HVDC system, it should be usually improve the control system effectiveness and also choose good strategy of control and this can lead to improve the performance of the system. A perfect strategy of control depends upon on a specific mathematical modeling for the VSC HVDC transmission [1].

PI regulator is a key element for control system uses, but it has the inconvenient of an enough control for improving the stability of the whole system during system operating condition. In order to limit the severity of this disadvantage, the selection of correct gains for the PI regulator is an obligation and this passes by finding new techniques to compute these adequate parameters [2]. Authors in [3,4,5] use different control system for VSC-HVDC link with different ways to find suitable PI controller parameters. Authors in [6] choose PSO method to ameliorate the VSC-HVDC stability but still it presents good convergence speed, obtained results have found with low accuracy. Authors in [7] regulate the gains of PI controller by FireFly Integrated-Sea Lion Optimization algorithm (FFI-SL<sub>NO</sub>) in which the results are compared to other traditional method. In [8] advanced Multivariable Proportional – Integral PI (SMPI) controller for VSP/HVDC interconnected system is used, the Swarm – Based Optimization Algorithms (SBOAs) in the tuning process of MPI controller, which is called swarm – based MPI (SMPI). PSO, GOA and GWO algorithms are used for tuning process of the designed SMPI. Authors in [9] presents a new swarm intelligence algorithm called bacterial foraging optimization whom is introduced to find the optimal parameters of the PI controller in which this approach offers great flexibility for the stability of the VSC-HVDC. In these previous works Meta-heuristic algorithms are used for optimization purpose. In other works, researchers relied on artificial intelligence methods such as fuzzy logic in [10], the predictive control model in [11]. Authors in [12, 13, 14] have relied on various methods such as Golden Section Search, Anti-Windup PI Controllers and passive control model in which they present the advantages and also the disadvantages of these methods for tuning process of the designed PI regulators.

Contrary to other methods studied in recent works [15,16,17, 18], Simplex method is a fast and direct algorithm that can be used to minimize a multidimensional objective function without constraints. This approach has the advantage of the necessity lack to compute the derivatives to move along an objective function contrary to gradient methods. This method has been used in several fields as engineering, statistic.....etc, because it has the advantage of the use simplicity. The aim from the proposed work is to present the simplicity of this method to select new PI regulator gains for the conception of robust and strong control system dedicated to VSC HVDC transmission.

## 2. Modeling of the VSC HVDC system

The VSC HVDC link has two VSC stations; one works as rectifier and the other automatically as inverter. The two stations are connected on the one hand by a DC cable on their continuous sides and on the other hand to two alternative networks through transformers.

Figure 1 shows a common configuration for a three-phase forced commutation VSC converter using IGBT valves with ant parallel diodes. Due to the polarity of the voltage on each IGBT element and the unidirectional given by the use of diodes, the current can be conducted for each bridge in both directions. DC capacitors provide a DC source which allows a large amount of energy to be stored [19].

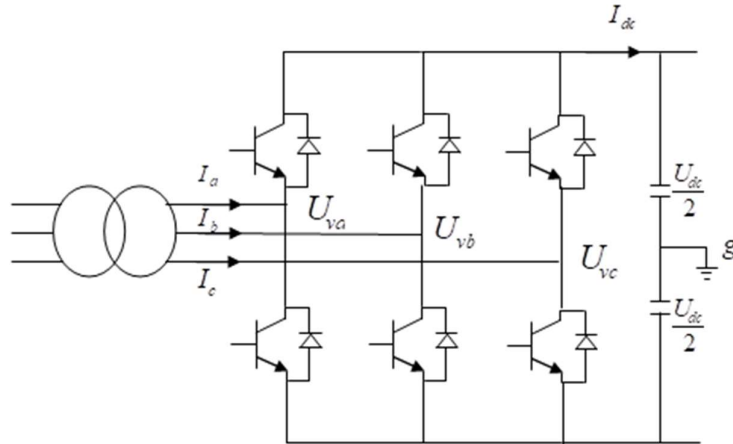


Fig. 1: Basic configuration of a VSC converter

The flow of the active and reactive power is established by the amplitude and angle between both vectors of the AC voltage of the connected network and the converter AC side voltage. The VSC scheme can be represented as a voltage source connected to an AC system via the combined impedances of the converter transformer and the series inductance as shown in Figure 2.

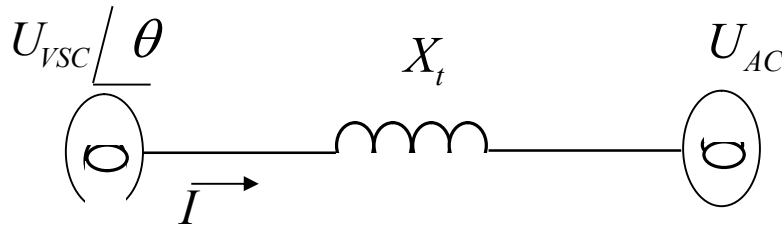


Fig. 2: Representation of voltage angle and impedance

The active power  $P$  from the VSC converter to the AC network can be expressed by:

$$p = \frac{U_{AC} U_{VSC}}{X_t} \sin(\theta) \quad (1)$$

The reactive power is given:

$$Q = \frac{U_{VSC} (U_{VSC} - U_{AC} \cos(\theta))}{X_t} \quad (2)$$

Where:  $U_{AC}$ : is the AC network voltage,  $U_{VSC}$  is the AC voltage of the VSC converter;  $X_t$  is the reactance between the VSC converter and the AC network and  $\theta$  indicates the voltage angle between the VSC converter and the AC network.

From these equations it can be seen that for no voltage angle difference, the real power is zero and the reactive power is determined by the difference in voltage magnitudes.

If  $U_{SYS} > U_{VSC}$ ,  $Q$  is less than zero and involves inductive operation (VSC absorbs reactive power).

If  $U_{VSC} > U_{SYS}$ ,  $Q$  is greater than zero and involves capacitive operation (VSC delivers reactive power to the grid).

For equal magnitudes of voltage, the reactive power is zero and the real power is determined by the voltage angle between the two vectors. If  $\delta > 0$ , power flows from VSC to AC system (inverter operation) and if  $\delta < 0$ , power flows from the AC system to the VSC (rectifier operation).

From the active and reactive power flow equations 1 and 2, it has been shown that four quadrant power control is possible and although active and reactive power can be controlled almost independently, there is a some measure of coupling introduced by the VSC scheme itself, as well as the connected AC systems. For reactive power control, the modulation index controls the amplitude of the AC voltage and the flow of reactive power and the ignition timing of the valves in relation to the AC side voltage determines the phase angle of voltage and power flow.

For the voltages and currents shown in Figure 3, the converter equations can be defined:

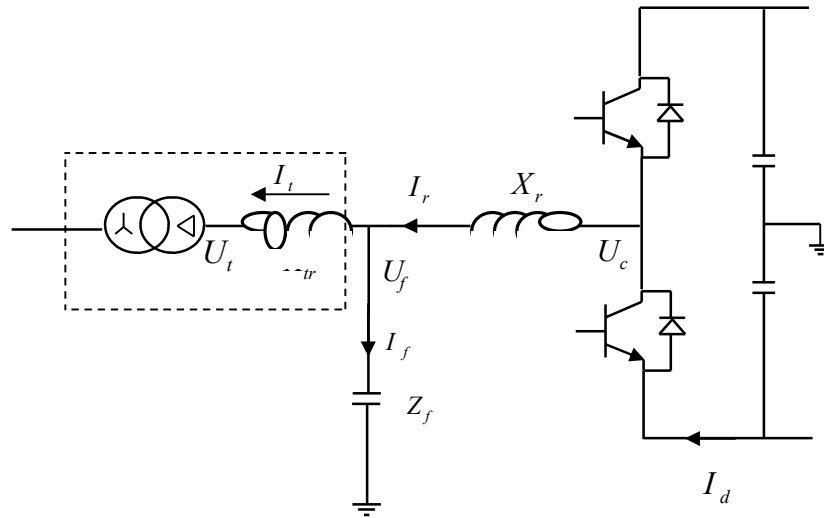


Fig. 3: Equivalent diagram of VSC circuit

The voltage of the converter is given by the relation:

$$U_c = U_f + X_r I_r \quad (3)$$

Where  $U_f$  is the AC filter node voltage,  $X_r$  is the reactance of the inductance of the converter and  $I_r$  is the current flowing through the inductance of the converter.

The current  $I_r$  is given by the relation:

$$I_r = I_t + I_f \quad (4)$$

Where  $I_t$  is the total current through the converter transformer and  $I_f$  is the current through the impedance of the filter.

The AC filter node voltage is given by the relationship:

$$U_f = U_t + X_r I_t \tag{5}$$

Where  $U_t$  is the voltage on the primary side of the converter transformer and  $X_{tr}$  is the reactance of the converter transformer.

The filter current is given by the following relation:

$$I_f = \frac{U_f}{Z_f} \tag{6}$$

The converter equations defined in equations (3) – (6) are represented by a vector diagram in Figure 4.

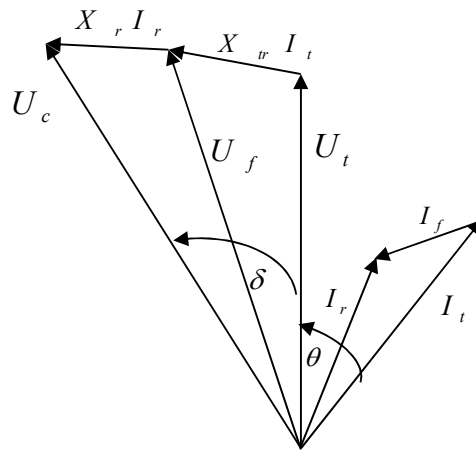


Fig. 4: Vector Representation of VSC Circuit

From figure 4,  $U_c$  can be equal to converter voltage  $U_{VSC}$  and  $U_t$  at system voltage  $U_{SYS}$  without the ratio of transformer and tap changer. The angle  $\delta$  is the voltage angle across the converter inductance and the transformer impedances and  $\theta$  is the angle between the output voltage and the current.

The inverter is composed of a voltage converter (VSC), as shown in Figure 5. The converter is connected between a capacitor of value  $C_I$ , which stabilizes the DC voltage needed for the VSC, and a step-up transformer.

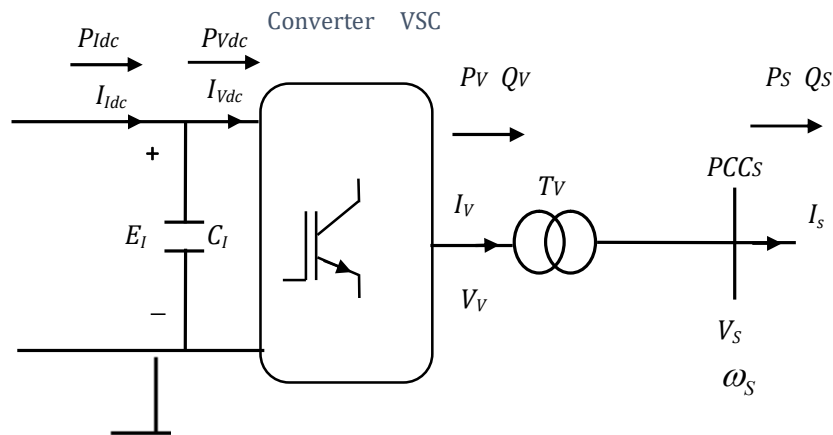


Fig. 5: Converter VSC

### 3. Control of the VSC HVDC system

The VSC HVDC control system has an inner current regulation loop controlling the AC currents. AC current references are given by outer regulators. On one hand the outer control loops contain the DC voltage and the AC voltage control at the receiving station and on the other hand contain the active power and the reactive power control at the sending station [20]. The control mode used in the system based on the use of PWM converter which permits to applied independent control at each side of the DC link [21]. At the sending station, the active power control is obtained by regulating the AC voltage phase angle and the reactive power is controlled around zero value by regulating the AC voltage magnitude.

At the receiving station the AC voltage phase angle is regulated in order to control the dc voltage of the DC link. This strategy of control is well detailed in [15, 22, 4]. An optimization strategy based on Simplex method is added to the control systems in each station as presented in figure 6.

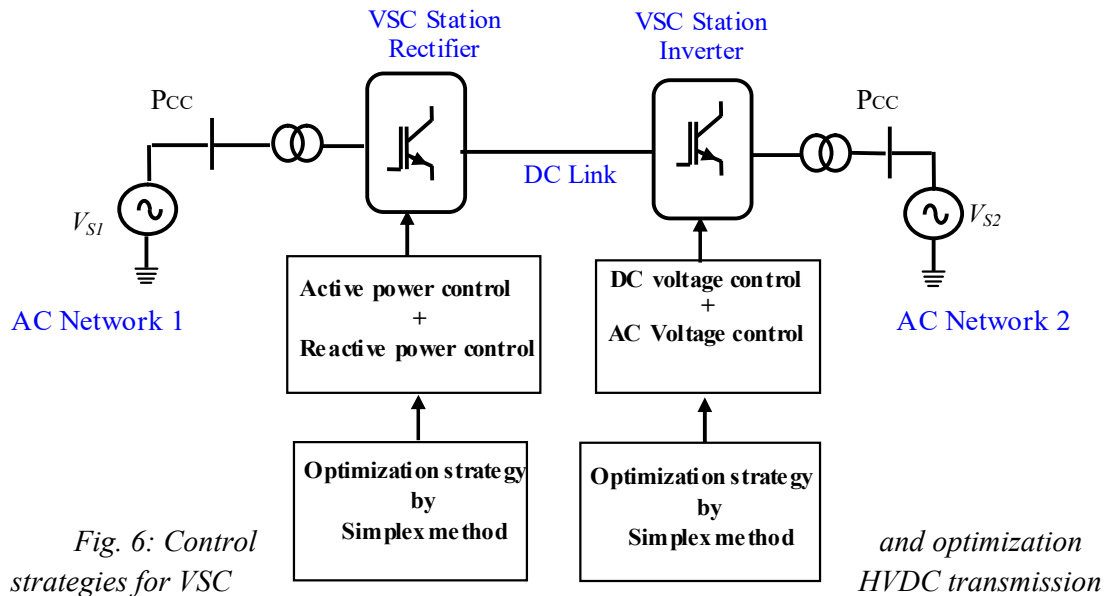


Fig. 6: Control strategies for VSC

and optimization HVDC transmission

#### 3.1 Control of the converter VSC currents

To control the currents of the VSC inverter, a strategy is used where the axes are oriented with the voltage \$V\_S\$, so \$V\_{Sd}=0\$. The input voltages are defined:

$$u_{vd} = \frac{1}{L_V} (V_{vd} + \omega_S L_V I_{Vq} - V_{Sd}) \quad (7)$$

$$u_{Vq} = \frac{1}{L_V} (V_{Vq} - \omega_S L_V I_{Vd}) \quad (8)$$

The following transformer equations \$T\_V\$:

$$u_{vd} = \frac{R_V}{L_V} I_{Vd} + \frac{dI_{Vd}}{dt} \quad (9)$$

$$u_{Vq} = \frac{R_V}{L_V} I_{Vq} + \frac{dI_{Vq}}{dt} \quad (10)$$

The transfer functions of these systems are as follows:

$$I_{Vd}(s) = \frac{1}{s + \frac{R_V}{L_V}} u_{Vd}(s) \quad (11)$$

$$I_{Vq}(s) = \frac{1}{s + \frac{R_V}{L_V}} u_{Vq}(s) \quad (12)$$

So first-order systems that can be controlled by PI regulators. Figure 7 shows the current control of the VSC converter. Limits are included in the currents to protect system components.

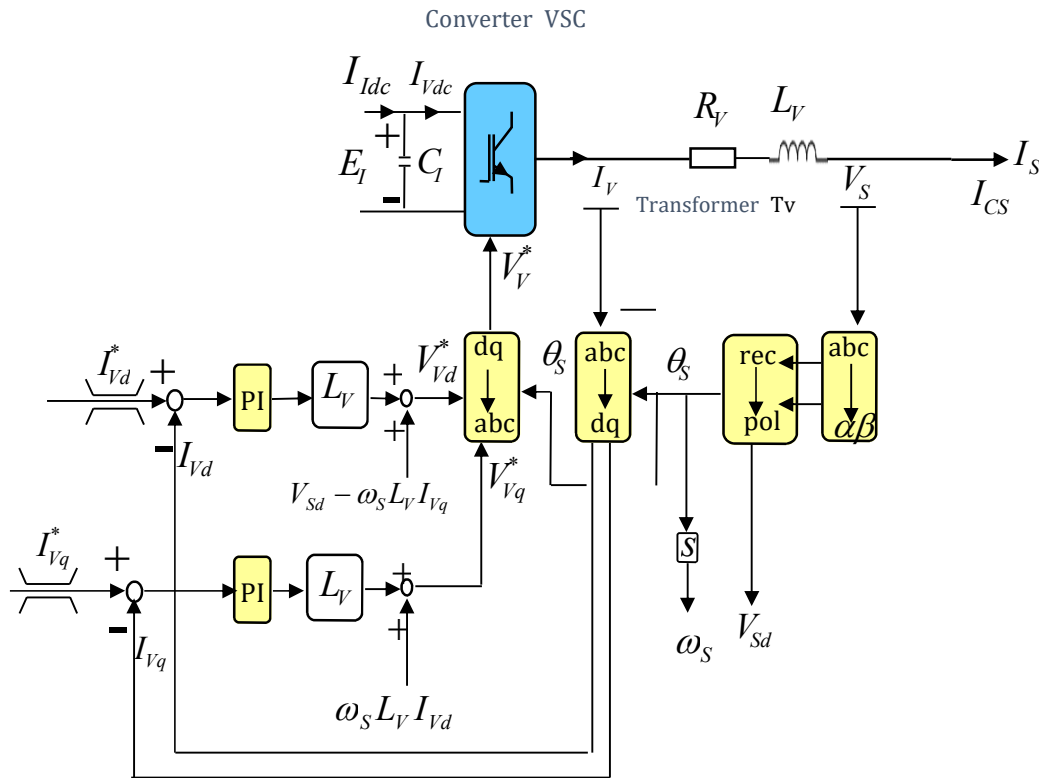


Fig. 7: Block Diagram of VSC Converter Current Control

#### 4. Strategy of optimization

In this work, the optimization strategy is based on the use of the Simplex method for the design of a new PI regulator more efficiency for improving the control system effectiveness.

##### 4.1- Simplex optimization method

Nelder and Mead -Simplex method is a method of optimization based on numerical respects [23]. Generally the aim from the use of this method is to find a function of n variables. For optimization, this function is habitually the objective function and it should be found with

minimum value [24]. The minimum objective function can be obtained when the simplex is moved directly to the optimal point [25]. This iterative process can be classified in these steps: reflection, contraction, expansion and reduction, but firstly the center of gravity should be computed.

**Center of gravity:** First, the vertices are ordered related to the objective function as follows:

$$F(X_1) \leq F(X_2) \leq F(X_3) \dots F(X_n) \leq F(X_{n+1})$$

The center of gravity is computed but the worst point for the objective function is excluded. It can be found from the following relation [15]:

$$C = \frac{1}{n} \sum_{i=1}^n X_i \quad (13)$$

**Reflection:** The reflection point  $X_r$  is computed from the following relation:

$$X_r = 2C - X_{n+1} \quad (14)$$

The value of the corresponding  $F$  at this reflected point is computed. If  $F(X_1) \leq F(X_r) \leq F(X_n)$ , the reflection point is better or equal to the  $n$  worst vertex.

In this case we replace  $X_{n+1}$  by  $X_r$  if no we go to the external contraction step.

**Expansion:** If  $F(X_r) < F(X_1)$  the expansion point is computed from this relation:

$$X_e = 2X_r - C \quad (15)$$

If  $F(X_e) < F(X_r)$ , the current best point is worse than this expansion point,  $X_e$  is replaces  $X_{n+1}$ . Otherwise,  $X_r$  replaces  $X_{n+1}$  and we go to the 2<sup>nd</sup> iteration.

**External and internal contraction:** if  $F(X_n) \leq F(X_r) < F(X_{n+1})$ , the external contraction is carried out using point  $X_r$ , The point of the external contraction is defined as follows:

$$X_{C_{ext}} = \frac{1}{2}(X_r + C) \quad (16)$$

If  $F(X_{oc}) \leq F(X_r)$ ,  $X_{oc}$  replaces  $X_{n+1}$  and we go to the 2<sup>nd</sup> iteration if no we go to the **Shrinkage** step.

If  $F(X_{n+1}) \leq F(X_r)$ , the internal contraction is carried out using point  $X_r$ . The point of the internal contraction is defined as follows:

$$X_{C_{int}} = \frac{3}{2}C - \frac{1}{2}X_r \quad (17)$$

If  $F(X_{ic}) < F(X_{n+1})$ ,  $X_{n+1}$  is replaced by  $X_{ic}$  and we go to the 2<sup>nd</sup> iteration, if no we go to the **Shrinkage** step.

**Shrinkage:** During this operation,  $n$  new vertices are computed as follows:

$$X_i = X_i + \frac{1}{2}(X_i - X_1) \quad (18) \text{ For}$$

$i = 2 \dots n + 1$ . This simplex is accepted and the conversion is completed.

### Algorithm

**For the first iteration:**

1- **Reorder the objective function  $F$  at the vertices from 1..to  $n+1$  such as:**

$$F(X_1) \leq F(X_2) \leq F(X_3) \dots F(X_n) \leq F(X_{n+1})$$

2- **Compute the Center of gravity from equation (3) Excluding  $X_{n+1}$**



- 3- **Reflection:** compute the reflection point  $X_r$  from equation (4)  
 If  $F(X_1) \leq F(X_r) \leq F(X_n)$  replace  $X_{n+1}$  with  $X_r$
- 4- **Expansion:** if  $F(X_r) < F(X_1)$ , compute the expansion point  $X_e$  from equation (5)  
 If  $F(X_e) < F(X_r)$  replace  $X_{n+1}$  with  $X_e$  otherwise replace  $X_{n+1}$  with  $X_r$
- 5- **Outside contraction:** if  $F(X_n) \leq F(X_r) < F(X_{n+1})$ , compute the outside contraction point  $X_{oc}$  from equation (6)  
 If  $F(X_{oc}) \leq F(X_r)$  replace  $X_{n+1}$  with  $X_{oc}$  and pass to the second iteration otherwise go to shrinkage step
- 6- **Inside contraction:** if  $F(X_{n+1}) \leq F(X_r)$  compute the inside contraction point  $X_{ic}$  from equation (7)  
 If  $F(X_{ic}) < F(X_{n+1})$  replace  $X_{n+1}$  with  $X_{ic}$  and pass to the second iteration otherwise go to shrinkage step
- 7- **Shrinkage:** n new vertices are computed from equation (8) with  $i=2, \dots, n+1$ . This simplex is accepted and the conversion is complete.

**4.2 The Simplex method for control system optimization**

In order to ameliorate the PI regulators performance during normal functioning and also against any disturbances that may occur, the parameters of these regulators will be computed using Simplex algorithm. The objective function is always the problem concerned by the optimization and the mathematical model of the objective function must be carefully selected [26]. For this purpose, the control system performance is evaluated by the ISE criterion (the integral of the error square). The ISE index is expressed as follows:

$$J_{ISE} = \int_0^T e(t)^2 dt \tag{19}$$

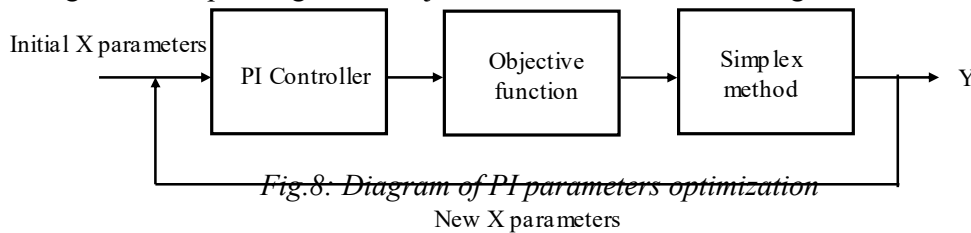
The objective of using this performance criterion is to correct control systems with long-lasting transient conditions and much less account for the overshoot of 1 [27]. According to this criterion, the design of the objective function is as follows:

$$Q_f(X) = \sum_{i=1}^6 \int_0^T (e_i)^2 dt \tag{20}$$

Where  $e(t)$ : is the error between the desired value the existent one, i presents the index of the regulator. And:

$$X = K_{P1}, K_{P2}, K_{P3}, K_{P4}, K_{P5}, K_{P6}, T_{i1}, T_{i2}, T_{i3}, T_{i5}, T_{i6}$$

The diagram corresponding to this objective function is shown in Figure 8.



## 5. Results

For validating the optimization strategy described previously, simulation studies are carried out using the PSCAD software. The time of computation is around some minutes to one hour. Figure 9 shows VSC HVDC transmission with the principal electrical parameters.

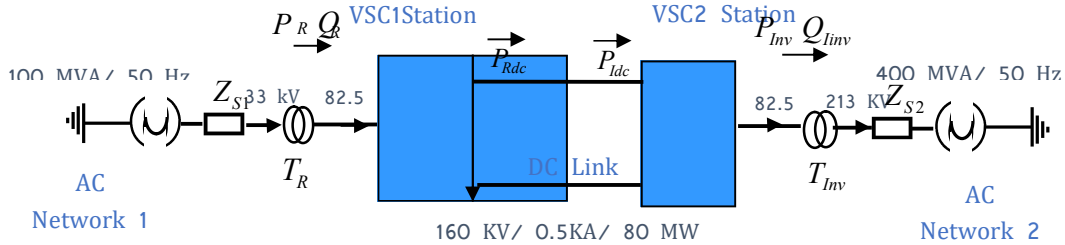


Fig.9: VSC HVDC System

For confirming the PI regulators efficacy, test simulations are performed to validate the application of the Simplex approach. Simulation tests include transient responses applied in some PI regulators in both sides of the link.

### 5.1- Step changes in reactive power reference at VSC rectifier side

A transient response is simulated when operating in nominal functioning at the moment  $t = 2$  s, where the reference of the reactive power is increased in ramp of 0.4 pu then it is decreased in ramp of the same quantity at the instant 3 s. After the simulation execution, the new parameters which are quoted with the other initials for the external control loop of the reactive power as follows:

Table 01: PI parameters

PI Gains	Kp	Ki	Objective Function
Before optimization	1.5	0.9	1.6406
After optimization	1.45873	0.03251	1.15325

The results are shown in figures 10, 11 and 12. It is clear from figures 10 and 11 that the reactive power follows well its reference after optimization by Simplex method compared to that with initial values for the regulator. So it is clearly noticed that the simplex method has a great success for developing the system functioning during the applied response step.

The increase on  $Q_R$  produces a decrease in the AC voltage  $V_R$  (0.82 pu) at rectifier side due to the capacitive nature of the AC grid as shown in figure 12 but the AC voltage  $V_{in}$  at inverter AC side is constant around its rated value. Also this figure presents small variations in DC current and also in DC voltages during the step application because of the converters effect. This type of response has tiny effects in the parameters of the DC link and also in the other AC side of the link.

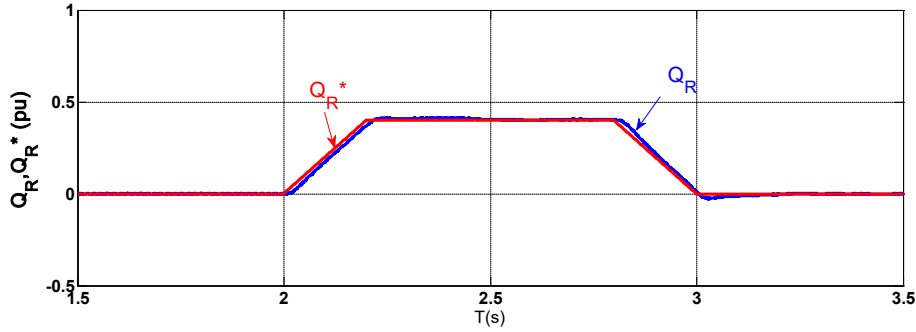


Fig. 10: Reactive power during positive response step after optimization

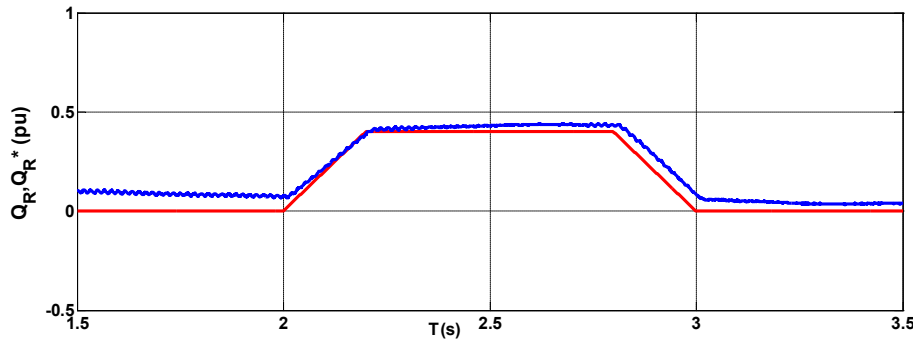


Fig. 11: Reactive power during positive response step before optimization

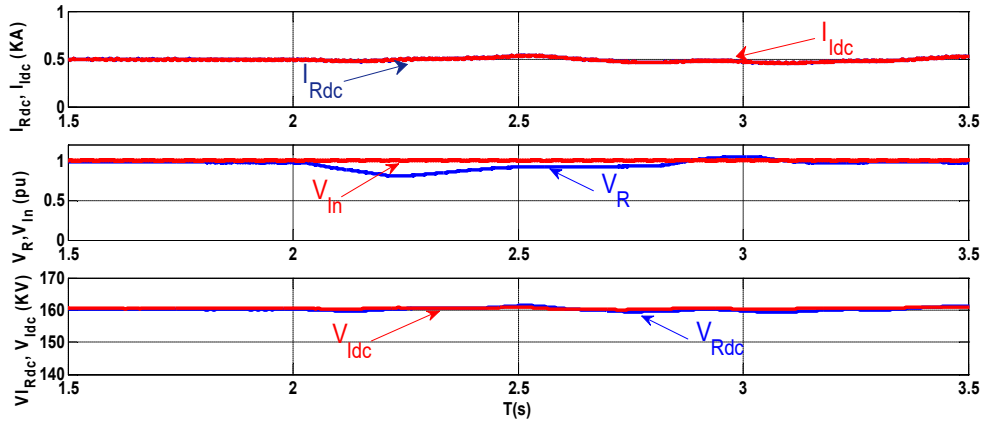


Fig. 12: DC currents and voltages, AC voltages during positive response step applied at  $Q_R^*$

**5.2- Step changes in DC voltage reference at VSC inverter side**

At VSC inverter DC side, a negative step in ramp is applied to the reference of the DC voltage at the moment 4 s for duration of 1s. The new gains of the regulator are cited in the following table:

PI Gains	Kp	Objective Function
Before optimization	0.6014	1.13902
After optimization	1.21377	0.688979

In figure 13 after optimization, the real voltage follows very well the DC reference voltage during, whereas in figure14 the real and reference voltages have the same behavior. From figure15, the DC voltage VRDC of the link has the same behavior with VIdc and the AC voltages in each side have small variations. In figure 16, it seems that at the step beginning and end, huge transients in DC powers are observed and also in DC currents because of the DC capacitor size.

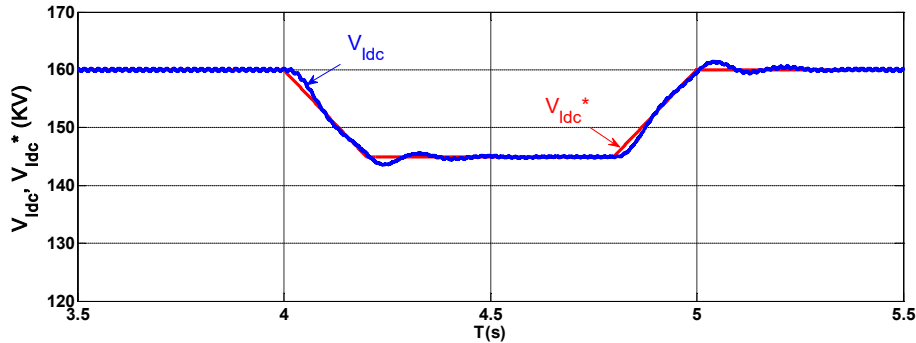


Fig.13: DC voltage of the link HVDC during negative response step after optimization

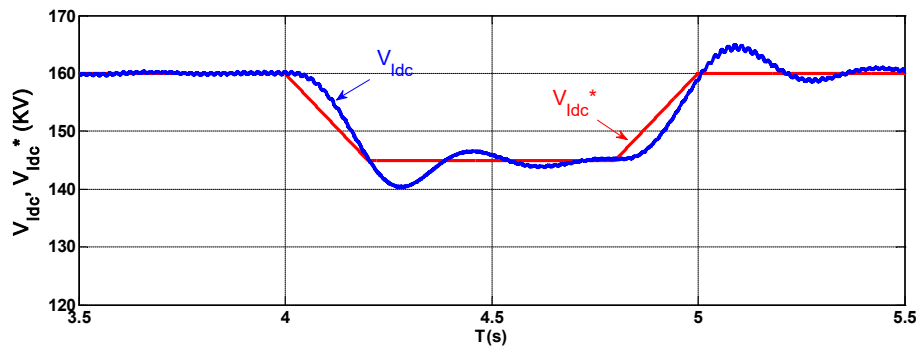


Fig.14: DC voltage of the link HVDC during negative response step before optimization

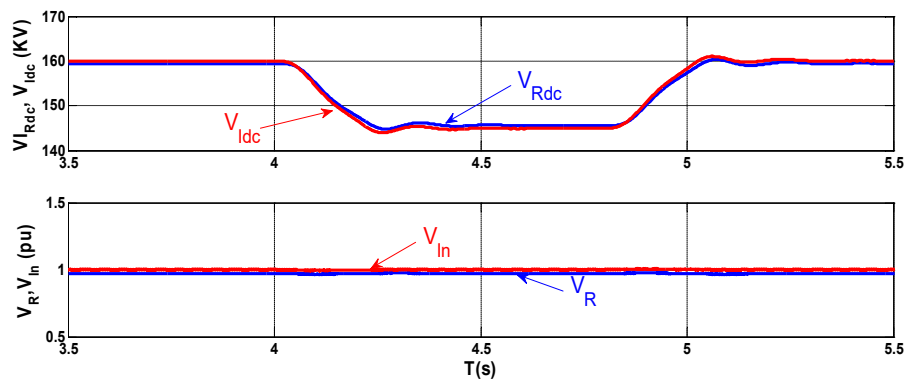


Fig. 15: DC voltages, AC voltages during negative response step applied at  $V_{Idc}^*$

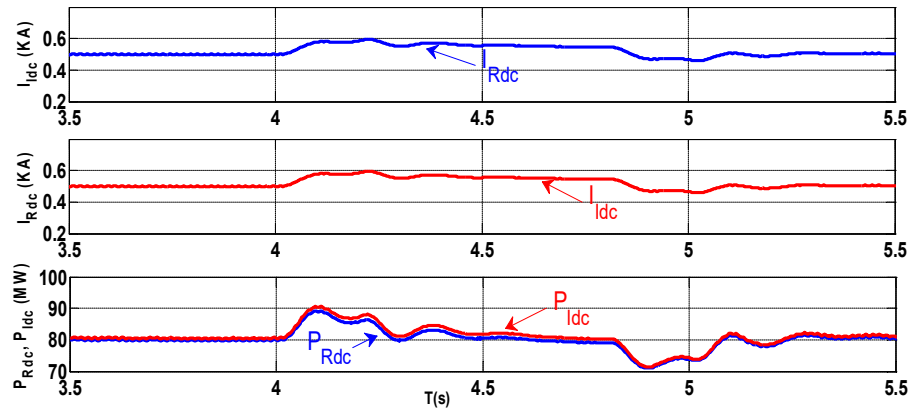


Fig. 16: DC currents, DC powers during positive response step applied at  $V_{Idc}^*$

### 5.3- Step changes in AC voltage reference at VSC rectifier side

At the moment  $t = 3$  s, a negative step of 0.3 pu is applied to the value of the AC voltage reference for duration of 0.8 s, then it is increased up to 1 pu at the instant  $t = 3.8$  s. After the simulation execution, we obtain the new parameters which are quoted with the other initials for the external control loop of the AC voltage as follows:

Table 02: PI parameters

PI Gains	$K_p$	$K_i$	Objective Function
Before optimization	1.2	0.1	1.04276
After optimization	1.25621	0.01248	0.864352

Figures 17 and 18 show the response of the system to changes in the AC voltage reference. The two figures show a comparison between two simulation results. After optimizations, the real AC voltage pursues its reference during the application of the step compared to the result before optimization. Figure 19 presents clearly that the inverter delivers the necessary reactive power to the AC grid during the response step while the reactive in the other side of the link is kept around its rated value. Also this figure shows the behavior of the AC voltage at rectifier side in which it keeps its rated value (1 pu).

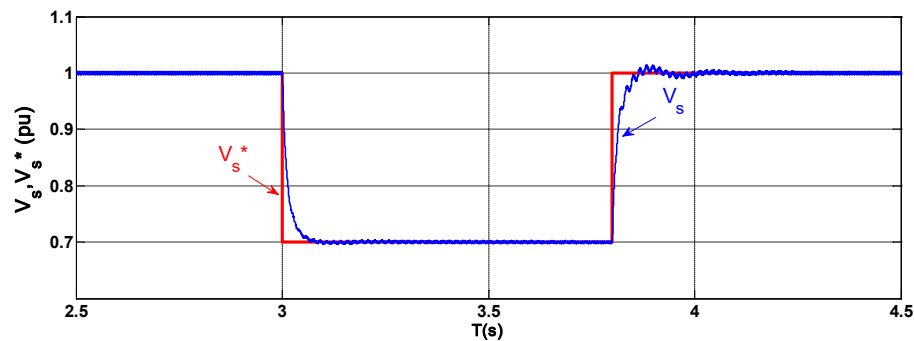


Fig.17: AC voltage at inverter side during negative response step after optimization

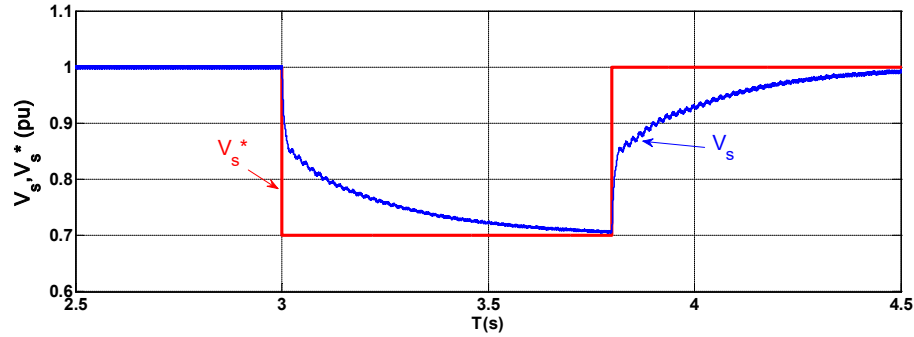


Fig.18: AC voltage at inverter side during negative response step before optimization

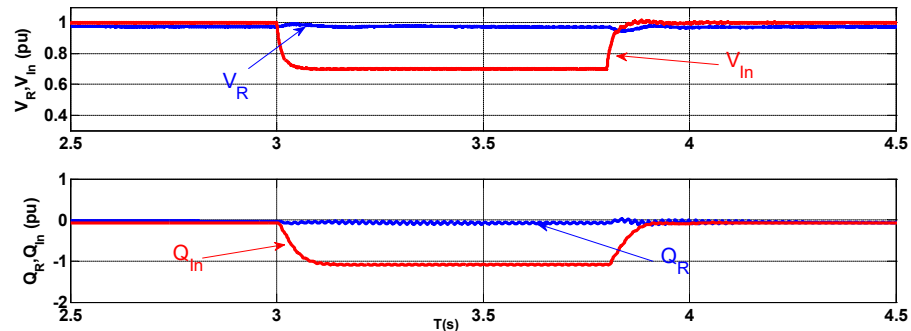


Fig. 19: Reactive powers, AC voltages during negative response step applied at  $V_{in}^*$

## 6- Conclusion

In this work, the control strategies proposed mainly use PI controllers optimized by the Simplex method. This approach has been introduced into the control system for each used regulator. This algorithm has the advantage of perfect accuracy and typical speed for finding new PI parameters from others derived from a conventional method. The Simplex approach improves the performance of the control system chosen for the HVDC system. Also the behavior of the HVDC link is well analyzed during the application of transient responses. As future work the synergy of this approach with the Hooke Jeeves method or the comparison between them can be studied as an interest subject.

## References

- [1] Chaudhary, S. K., Teodorescu, R., Rodriguez, P., Kjær P. C. "Chopper controlled resistors in VSC-HVDC transmission for WPP with full-scale converters", In: IEEE PES/IAS Conference on Sustainable Alternative Energy, Valencia, Spain, Sept. 28-30, 2009, pp. 1-8.
- [2] Chengyong, Z., Xiangdong, L., Guangkai, L.: Parameters Optimization of VSC-HVDC Control System Based on Simplex Algorithm. In: proceedings of Power Engineering Society General Meeting, IEEE. June. 24-28, 2007, Tampa, USA, P.1 - 7.
- [3] Bajracharya, C.: Control of VSC-HVDC for wind power. Master thesis June 2008. Norwegian University of Science and Technology, Norway, 2008.

- [4] Haileselassie TM, Torres-Olguin RE, Vrana TK, Uhlen K, Undeland T (2011) Main grid frequency support strategy for VSCHVDCconnected wind farms with variable speed wind turbines. In: Proceedings of the Power Tech. IEEE Press, Trondheim, pp 1–6
- [5] Irina Stan A, Ioan Stroe D (2010) Control of VSC-based HVDC transmission system for offshore wind power plants. Master thesis. Aalborg University, Denmark
- [6] Nayak N, Rout Ray SK, Rout PK (2011) Improvement of transient stability of VSC-HVDC system with particle swarm optimization based PI controller. *Int J Power Syst Oper Energy Manag (IJPSOEM)* 1(1):81–89
- [7] G.D.K.N.S.Thankachy, S.Therese, P.Raj, “Design of optimized PI controller for 7-level inverter: a new control strategy”, *Environmental Science and Pollution Research*, Edition 2021.
- [8] Elyas.R, Iman.M.H.N, Hasan.M, “Comparative study of SBOAs on the tuning procedure of the designed SMPI controller for MIMO VSP/HVDC interconnected model”, *International Journal of Electrical Power and Energy Systems*, Volume 129, Edition 2021.
- [9] L.Mazouz, S.A Zidi, M Khatir, S Saadi, T Benmassaoud. ‘ Particle Swarm Optimization based PI controller of VSC-HVDC system connected to a wind farm’, *International Journal of System Assurance Engineering and Management*, , Volume 7, Supplement 1, pp 239–246, December 2016.
- [10] S.A.Khan, C.Liu, J A Ansari, “Centralized Fuzzy Logic Based Optimization of PI Controllers for VSC Control in MTDC Network”, *Journal of Electrical Engineering & Technology*, Volume 15, Edition 2020.
- [11] M.I.Hossain, M.Shafiullah, M. Abldo, “VSC Controllers for Multiterminal HVDC Transmission System: A Comparative Study”, *Arabian Journal for Science and Engineering*, Volume 45, Edition 2020.
- [12] R. Agarwal, S Singh, “Optimized Controller Design for a 12-Pulse Voltage Source Converter Based HVDC System”, *Journal of The Institution of Engineers (India)*, Volume 98, Edition 2017.
- [13] M.A.A.Murad, M.Liu, Member IEEE & F.Milano, Fellow IEEE, “Modeling and Simulation of Variable Limits on Conditional Anti-Windup PI Controllers for VSC-Based Devices”, *IEEE TRANSACTIONS ON CIRCUITS AND SYSTEMS*, VOL. 68, NO. 7, JULY 2021.
- [14] Y.Li, J.Guo, Xi Zhang , Member, IEEE, S.Wang, S.Ma, Member, IEEE, B.Zhao, G.Wu, Member, IEEE, and T.Wang “Over-Voltage Suppression Methods for the MMC-VSC-HVDC Wind Farm Integration System”, *IEEE TRANSACTIONS ON CIRCUITS AND SYSTEMS*, VOL. 67, NO. 2, FEBRUARY 2020.
- [15]L Mazouz, S.A. Zidi, S Saadi, T Benmassaoud, M Elaguab. “Hybrid Swarm Intelligence Approach Based PI Regulator for VSC-HVDC Optimal Parameters” *Journal of Electrical Engineering, Romania*, Volume 14, Edition : 2, 2014.
- [16]L. Mazouz, S.A. Zidi, S. Saadi, M. Khatir, T. Benmassaoud. “VSC-HVDC system optimized PI controllers using bacterial foraging algorithm” *journal of electrical engineering springer*, Volume 97, Issue 3, pp 205–212, Germany, September 2015.
- [17]Z. Jia and Che. Zhao “Parameters Optimization of HVDC Control System Based on Simplex Algorithm in RTDS” 2010 IEEE 5th International Conference on Critical Infrastructure (CRIS) Pages: 1 - 6, 2010.

- [18] L. Mazouz, S.A Zidi, A Hafaifa, S Hadjeri, T Benaissa. ,," Optimal regulators conception for wind turbine PMSG Generator using Hooke jeeves method""", Periodica Polytechnica Electrical Engineering and Computer Science, accepted 20-02- 2019.
- [19] M. P. Bahrman "Overview of HVDC transmission" PSCE, pp. 18-23, 2006.
- [20] Xinming F, Lin G, Chengjun X, Jianming H (2013) A passivity control strategy for VSC-HVDC connected large scale wind power. In: Proceedings of Innovative Smart Grid Technologies (ISGT), IEEE Press, Washington, DC, pp 1–6
- [21] PSCAD User Guide.
- [22] Lie, X., Yao, L., Bazargan, M., Yi, W.: The Role of Multiterminal HVDC for Wind Power Transmission and AC Network Support. In: Proceedings of the Power and Energy Engineering Conference, IEEE. March 28-31, 2010, Chengdu, China, Page(s): 1 – 4.
- [23] N. Pham, Bogdan M. Wilamowski "Improved Nelder Mead's Simplex Method and Applications" Journal of Computing, Volume 3, Issue 3, March 2011.
- [24] A. Andersson "Optimized Tuning of Parameters for HVDC Dynamic Performance Studies" Master thesis, UPPSALA University, Sweden, 2013.
- [25] S. Filizadeh, A. M. Gole, D. A. Woodford, and G. D. Irwin, "An optimization-enabled electromagnetic transient simulation-based methodology for HVDC controller design" IEEE Transactions on Power Delivery, vol. 22, no. 4, pp. 2559-2566, 2007.
- [26] Kealy, T., Dwyer, O. "A. Analytical ISE Calculation and Optimum Control System Design", In: Irish Signals and Systems Conference, Limerick, Ireland, July, 2-3, 2003, pp. 265-273. [online] Available at:  
<https://arrow.dit.ie/cgi/viewcontent.cgi?article=1145&context=engscheleart>
- [27] I. Chalane T. Ouari "Optimisation des paramètres d'un PID par essais particuliers (PSO)." Master Thesis, University Of Bejaia, Juin 2017.